The Lomax Distribution for Wireless Channel Modeling: Theory and Applications

IVAN SÁNCHEZ [1,2] **AND F. JAVIER LÓPEZ-MARTÍNEZ** [1,3] **(Senior Member, IEEE)**

[1]Communications and Signal Processing Lab, Telecommunication Research Institute (TELMA), Universidad de Málaga, 29010 Málaga, Spain
[2]Department of Telecommunication Engineering, Universidad de las Américas, Quito 170503, Ecuador
[3]Department Signal Theory, Networking and Communications, Research Centre for Information and Communication Technologies (CITIC-UGR), University of Granada, 18071 Granada, Spain

CORRESPONDING AUTHOR: IVAN SÁNCHEZ (e-mail: ivan.sanchez.salazar@uma.es)

ABSTRACT We investigate the application of the Lomax distribution for wireless fading modeling purposes. By a proper redefinition of its scale parameter, we present closed-form expressions for its main statistics: probability density function, cumulative distribution function, raw moments and Laplace-domain statistics. Then, relevant performance indicators are derived, including the amount of fading, channel capacity, outage probability and error rate. Other applications include diversity reception using selection combining, as well as composite fading modeling. The Lomax distribution is compared to the relevant case of Rayleigh fading, and to other benchmark distributions of similar complexity used in the literature.

INDEX TERMS Fading channels, Lomax distribution, performance analysis, wireless communications.

I. INTRODUCTION

Radio signals used to transmit information experience a number of effects when traversing the wireless medium, including attenuation, delay, scattering, diffraction, and many others. The characterization of these aggregate effects over the desired information signal is referred to as channel modeling. While an exact model for such channels is very challenging due to the complexity of the problem, e.g., based on Maxwell equations and electromagnetic laws [2], some simplified models are of widespread use in the literature. For instance, this is the case of the Gaussian models like Rayleigh and Rice [3], inspired in the central limit theorem due to the reception of a large number of scattered waves.

However, since radio propagation is far more involved than what these simplified models are able to capture, the literature is rich in other alternatives for stochastic wireless channel modeling [4], [5], [6], [7], [8], [9]. In these aforementioned cases the resulting distributions are based on some propagation effects such as clustering, line-of-sight fluctuation, or other effects. In general terms, the two dominant approaches for wireless channel modeling can be categorized as *ray-based* and *cluster-based*. In the former, the received signal is

modeled as a coherent sum of incident waves, each of these with a different amplitude and phase. In the latter, the received signal is structured into clusters of waves, where each cluster is composed by groups of scattered waves with similar delays. Ray-based formulations include popular fading models in the literature suc as Durgin's Two-Wave with Diffuse Power (TWDP) [10] and other generalizations [11], [12], [13], [14]. On the other hand, cluster-based models include Yacoub's κ-μ and η-μ models [6], ans subsequent extensions [8], [15], [16], [17], [18], [19].

Besides these two approaches based on an underlying physical model for propagation, there exist a third way to statistical channel modeling: since radio propagation mechanisms are very complex to be accurately modeled in every possible situation, sometimes the use of certain distributions borrowed from statistics may be justified based on goodness of fit to experimental data, or even its mathematical simplicity. This is the case, among others, of the Weibull [20], [21], inverse-gamma [22], [23], Log-Logistic [24] distributions. Interestingly, after their definition and extensive use by the research community, these somehow unconventional models may even be connnected to an underlying physical

mechanism. For instance, the Weibull model is connected with an underlying Rayleigh model affected by a non-linear transformation, and even admits further generalizations based on this premise [7].

Digging a bit deeper into the literature, the Lomax[1] distribution has also been considered by some authors as a candidate for wireless channel modeling [25], [26]. At first glance, the use of such a distribution may seem unconventional from a physical perspective. However, the authors in [26] connect the Lomax distribution with an underlying complex signal distributed according to a joint T-distribution, being its uncorrelated real and imaginary parts Lomax distributed. This is also related to a Rayleigh-like propagation condition affected by parametric uncertainty due to finite sample size observation, which is relevant in ultra reliable and low-latency communications (URLLC) [27]. In the communications literature, the Lomax distribution has been used in a number of scenarios, including content delivery in device-to-device (D2D) communications [28], [29], bit error performance under interference [30], cooperative spectrum sensing in cognitive radio networks [31], [32], or URLLC [27], [33], [34].

Motivated by the above considerations, we conduct a formal analysis to enable the use of the Lomax distribution as a candidate to model fading in wireless channels. This requires a redefinition of its parameters, so that physical restrictions such as the existence of its first moment (i.e., the average received power) are properly included. In the sequel, we will use the shorthand notation $\mathfrak{L}_x$ distribution to refer to such a redefinition of the Lomax distribution. Closed-form expressions for its probability density function (PDF), cumulative distribution function (CDF), and raw moments are derived. Closed-form expressions are also obtained for relevant Laplace-domain statistics, including the moment generating function (MGF) and the generalized MGF (G-MGF). The performance of wireless communication systems operating under $\mathfrak{L}_x$ fading is exemplified, computing relevant performance metrics such as the outage probability (OP) and average channel capacity in exact and asymptotic form. Additional applications that highlight the potential of the $\mathfrak{L}_x$ distribution include error probability analysis, diversity reception through selection combining (SC), and composite fading modeling.

The remainder of this paper is organized as follows: The main statistics of the $\mathfrak{L}_x$ distribution are derived in Section II, and their application to derive performance metrics in communications is carried out in Section III. Numerical results are given in Section IV, whereas the main conclusions are outlined in Section V. The key definitions and notation are included in Table 1.

---

[1] connected to the Pareto Type II distribution.

TABLE 1 Notation and Definitions

Notation	Definition
$F_{(.)}(\cdot)$	Cumulative Distribution Function (CDF)
$f_{(.)}(\cdot)$	Probability Density Function (PDF)
$F_{(.)}^{-1}(p; \cdot)$	Inverse CDF (ICDF)
$M_\gamma(s)$	Moment Generating Function (MGF)
$M_\gamma^n(s)$	Generalized Moment Generating Function (G-MGF)
$\mathfrak{L}_x(\alpha, \lambda)$	Lomax distribution with parameters λ (scale) and α (shape)
$\mathcal{CN}(\mu, \sigma^2)$	Complex Gaussian distribution with parameters μ and σ^2
$\sim$	Statistically distributed as
i.i.d.	Independent and identically distributed
$\mathbb{E}\{\cdot\}$	Expectation operator
$\triangleq$	Defined as
$\log_2(\cdot)$	Base-2 logarithm
$\log(\cdot)$	Natural logarithm
$\Gamma(\cdot)$	Gamma function [34, Eq. (6.1.1)]
$U(\cdot, \cdot, \cdot)$	Confluent hypergeometric Tricomi function [35, Eq. (9.211)]
$\gamma_e = 0.57721\ldots$	Euler-Mascheroni constant [34, 6.1.3]
$\Psi(\cdot)$	Digamma function [34, 6.3.1]

II. STATISTICAL CHARACTERIZATION

In this section, we first present some preliminary definitions required for the subsequent analysis. Then, the main statistics of the $\mathfrak{L}_x$ distribution are introduced.

A. PRELIMINARIES

Definition 1 (Lomax distribution): Let $\gamma \sim \mathfrak{L}_x(\alpha, \lambda)$, i.e., a random variable following a Lomax distribution [37] with shape $\alpha > 0$ and scale $\lambda > 0$. The PDF of γ is given by

$$f_\gamma(\gamma) = \frac{\alpha}{\lambda} \left[1 + \frac{\gamma}{\lambda} \right]^{-(\alpha+1)}. \tag{1}$$

Definition 2 (Instantaneous SNR): Let z be the received signal at the destination node of a wireless communication system, so that

$$z = \sqrt{P_T S_T} hx + w, \tag{2}$$

with P_T representing the equivalent transmit power, S_T the aggregate losses (including path loss), h the normalized fading channel coefficient with $\mathbb{E}\{|h|^2\} = 1$, x the normalized transmitted symbol with $\mathbb{E}\{|x|^2\} = 1$, and w the additive white Gaussian noise (AWGN) term, $w \sim \mathcal{CN}(0, N_0)$. Then, the instantaneous signal-to-noise ratio (SNR) is given as

$$\gamma = \frac{P_T S_T |x|^2}{N_0} |h|^2, \tag{3}$$

so that $\overline{\gamma} \triangleq \mathbb{E}\{\gamma\} = P_T S_T / N_0$ is the average SNR.

B. MAIN STATISTICS OF THE $\mathfrak{L}_x$ DISTRIBUTION

We wish to formulate a model for the $\mathfrak{L}_x$ distribution that can be useful for the purpose of channel modeling. We will assume that the instantaneous SNR γ follows the $\mathfrak{L}_x$ distribution. However, it is customary that the average SNR $\overline{\gamma}$ explicitly appears as one of the distribution parameters. Now, since $\overline{\gamma} = \mathbb{E}\{\gamma\} = \frac{\lambda}{\alpha-1}$ from (1), we can express the scale parameter $\lambda = (\alpha - 1)\overline{\gamma}$. With this parameter redefinition, the

PDF of the $\mathfrak{L}_x$ distribution is reformulated in the following Lemma.

Lemma 1 (PDF): Let $\gamma \sim \mathfrak{L}_x(\alpha, \lambda)$, and let $\lambda = (\alpha - 1)\overline{\gamma}$. The PDF of γ is given by

$$f_\gamma(\gamma) = \frac{\alpha}{\overline{\gamma}(\alpha - 1)} \left[1 + \frac{\gamma}{\overline{\gamma}(\alpha - 1)} \right]^{-(\alpha+1)}, \qquad (4)$$

with $\overline{\gamma} > 0$ and $\alpha > 1$.

Proof: Substitution of $\lambda = (\alpha - 1)\overline{\gamma}$ completes the proof. $\square$

Compared to the expression in Definition 1, the PDF in Lemma 1 is only valid for $\alpha > 1$. This is due to the fact that, for $\alpha \leq 1$, the first-order moment of the $\mathfrak{L}_x$ distribution is not defined. Hence, the $\mathfrak{L}_x$ distribution only makes sense with $\alpha > 1$ for physical reasons, i.e., has a finite average received power or, equivalently, a finite average SNR. With this in mind, the CDF and the central moments of the $\mathfrak{L}_x$-distribution are given as follows.

Lemma 2 (CDF): Let $\gamma \sim \mathfrak{L}_x(\alpha, \lambda)$, and let $\lambda = (\alpha - 1)\overline{\gamma}$. The CDF of γ is given by

$$F_\gamma(\gamma; \alpha, \overline{\gamma}) = F_\gamma(\gamma) = 1 - \left[1 + \frac{\gamma}{\overline{\gamma}(\alpha - 1)} \right]^{-\alpha}, \qquad (5)$$

with $\overline{\gamma} > 0$ and $\alpha > 1$.

Proof: Direct integration of (4) yields (5). $\square$

Remark 1: With this redefinition of the Lomax distribution, the convergence in distribution to the exponential distribution can be easily proved. Taking the limit over the CDF as α goes to infinity, we have

$$\lim_{\alpha \to \infty} 1 - \left[1 + \frac{\gamma}{\overline{\gamma}(\alpha - 1)} \right]^{-\alpha} = 1 - e^{-\frac{\gamma}{\overline{\gamma}}}. \qquad (6)$$

Lemma 3 (Moments): Let $\gamma \sim \mathfrak{L}_x(\alpha, \lambda)$, and let $\lambda = (\alpha - 1)\overline{\gamma}$. The k-th non-central moment of γ is given by

$$\mathbb{E}\left\{\gamma^k\right\} = \overline{\gamma}^k \frac{(\alpha - 1)^k \, \Gamma(\alpha - k) \, \Gamma(1 + k)}{\Gamma(\alpha)}, \qquad (7)$$

with $\overline{\gamma} > 0$ and $\alpha > k$.

Proof: Using the definition of the raw moments, i.e., $\mathbb{E}\{\gamma^k\} = \int_0^\infty \gamma^k f_\gamma(\gamma) d\gamma$, after integration (7) is obtained. $\square$

From (7), the amount of fading (AoF) metric [38] is straightforwardly computed as per the next corollary.

Corollary 1 (AoF): Let $\gamma \sim \mathfrak{L}_x(\alpha, \lambda)$, and let $\lambda = (\alpha - 1)\overline{\gamma}$. The AoF of γ is given by

$$\text{AoF} = \frac{\mathbb{E}[\gamma^2]}{\overline{\gamma}^2} - 1 = \frac{\alpha}{\alpha - 2}, \qquad (8)$$

with $\overline{\gamma} > 0$ and $\alpha > 2$.

Proof: Using (7) and the well-known property of the gamma function $\Gamma(z + 1) = z\Gamma(z)$, then (8) is obtained after some manipulations. $\square$

Remarkably, the inverse CDF of the $\mathfrak{L}_x$ distribution can also be expressed in simple closed-form. This allows the

TABLE 2 Comparison Between Fading Models

Fading model	Closed-form statistics				
	PDF	CDF	MGF	GMGF	ICDF
Nakagami-m	✓	✓	✓	✓	*
Rician	✓	✓	✓	✓	✗
Weibull	✓	✓	✗	✗	✓
Hoyt	✓	✓	✓	✓	✗
Inverse Gaussian	✓	✓	✓	✓	✗
Folded-normal	✓	✓	✓	✓	✗
Log-logistic	✓	✓	✗	✗	✓
Lomax	✓	✓	✓	✓	✓

generation of uncorrelated samples through inverse transform sampling.

Lemma 4 (Inverse CDF): Let $\gamma \sim \mathfrak{L}_x(\alpha, \lambda)$, and let $\lambda = (\alpha - 1)\overline{\gamma}$. The inverse CDF of γ is given by

$$F_\gamma^{-1}(p; \overline{\gamma}, \alpha) = \overline{\gamma}(\alpha - 1)\left[(1 - p)^{-\frac{1}{\alpha}} - 1 \right], \qquad (9)$$

where $0 \leq p \leq 1$ denotes probability.

Proof: Finding γ in (5) yields (9). $\square$

The previous results allow for a complete characterization of the $\mathfrak{L}_x$ distribution in terms of relevant first order statistics. However, it is also possible to characterize this distribution in the Laplace domain, by computing some additional metrics related to the Moment Generating Function (MGF). Specifically, in the following theorem a closed-form expression for the generalized MGF (G-MGF) is derived:

Lemma 5 (G-MGF): Let $\gamma \sim \mathfrak{L}_x(\alpha, \lambda)$, and let $\lambda = (\alpha - 1)\overline{\gamma}$. The G-MGF of γ is given by

$$M_\gamma^n(s) = \alpha(\alpha - 1)^n \overline{\gamma}^n U(n + 1, n + 1 - \alpha, s(1 - \alpha)\overline{\gamma}). \qquad (10)$$

Proof: Using the definition of G-MGF as $M_\gamma^n(s) \triangleq \mathbb{E}\{\gamma^n e^{s\gamma}\}$, and using [36, 9.211.4] yields (11). $\square$

The G-MGF naturally appears when computing probability measures in several scenarios in communication theory: these include outage probability in interference limited scenarios [39], [40], physical layer security [41], energy detection [42], capacity analysis [43] or composite fading modeling [44]. This function also includes the conventional MGF as a special case, which is stated in the following corollary:

Corollary 2 (MGF): Let $\gamma \sim \mathfrak{L}_x(\alpha, \lambda)$, and let $\lambda = (\alpha - 1)\overline{\gamma}$. The MGF of γ is given by

$$M_\gamma(s) = \alpha U(1, 1 - \alpha, s(1 - \alpha)\overline{\gamma}). \qquad (11)$$

Proof: Setting $n = 0$ in (10) yields the desired result. $\square$

This brings additional benefits from a performance analysis perspective, since several performance metrics in wireless communications are expressed in terms of the MGF [38].

We now compare the $\mathfrak{L}_x$ distribution to other distributions used in the literature for wireless channel modeling. For a fair comparison, we only consider the cases of distributions with one shape parameter [21], [24], [45], [46], [47]. In the entries in Table 2, we indicate which of the relevant statistical functions are available in closed-form. We take the usual convention in the literature, which considers a *closed-form* as

that including a finite number of well-known functions [48]. This classically includes special functions like Bessel or Hypergeometric ones, but not more involved ones like Meijer-G of Fox-H functions. We note that one of the key benefits of the $\mathcal{L}_x$ distributions is that all five statistics admit a closed-form expression. This only happens with the Nakagami-m distribution, if we include the numerical implementation of its ICDF available in MATLAB or Mathematica within the closed-form definition (that's why the corresponding entry in Table 2 is marked with an asterisk). Even in otherwise tractable distributions such as the Rician and Folded-Normal ones, the CDF inversion needs to be implemented numerically [49].

III. APPLICATIONS

With the previous definitions and expressions in Section II, it is possible to carry out performance analysis of wireless communication systems operating under $\mathcal{L}_x$ fading channels. In the sequel, we will analyze a number of scenarios that include relevant performance metrics in wireless communications. These include outage probability (OP), channel capacity, error rate analysis and composite fading model. The effect of diversity under $\mathcal{L}_x$ fading is also evaluated, by considering the case of Selection Combining (SC) strategy.

A. OUTAGE PROBABILITY

The OP is defined as the probability that the instantaneous SNR falls below some threshold, i.e.,

$$\text{OP}\left(\gamma_{\text{th}}; \overline{\gamma}, \alpha\right) \triangleq \Pr\left\{\gamma < \gamma_{\text{th}}\right\} = F_\gamma(\gamma_{\text{th}}). \tag{12}$$

Hence, it can be straightforwardly evaluated from the distribution CDF in (5). Now, for sufficiently large values of average SNR, it is well-known that the OP admits a tight power law approximation $\text{OP} \approx G_c(\gamma_{\text{th}}/\overline{\gamma})^{G_d}$ [50] under some mild conditions. G_c is known as *power offset*, while G_d is referred to as *diversity order*. Taking a limit in (5), we can derive such an approximation for the case of $\mathcal{L}_x$ fading:

$$\lim_{\overline{\gamma} \to \infty} \text{OP}\left(\gamma_{\text{th}}; \overline{\gamma}, \alpha\right) = \text{OP}_{\text{asy}}\left(\gamma_{\text{th}}; \overline{\gamma}, \alpha\right) = \frac{\alpha\gamma}{\overline{\gamma}(\alpha-1)}. \tag{13}$$

We can identify $G_c = \frac{\alpha}{\alpha-1}$ as the power offset, and $G_d = 1$ as the diversity order of the $\mathcal{L}_x$-distribution. From (13), it can be easily seen that as α increases (i.e., as fading severity decreases), the OP is reduced. The OP analysis can be straightforwardly extended to the case of diversity reception. For this purpose, we consider the low-cost SC strategy, on which a multibranch receiver equipped with L receive antennas chooses the one with the largest SNR for reception. Mathematically, this can be expressed as:

$$\gamma_{\text{SC}} = \max_k \left(\gamma_k\right), \ k = 1 \ldots L. \tag{14}$$

Hence, the OP for the SC strategy is therefore given as [38]

$$\text{OP}_{\text{SC}}\left(\gamma_{\text{th}}; \overline{\gamma}, \alpha\right) = F_{\gamma_{\text{SC}}}(\gamma_{\text{th}}) = \left(F_\gamma(\gamma_{\text{th}})\right)^L, \tag{15}$$

where we assumed for simplicity the case with i.i.d. receive branches. The asymptotic CDF for the SC case can also be derived as

$$\lim_{\overline{\gamma} \to \infty} \text{OP}_{\text{SC}}\left(\gamma_{\text{th}}; \overline{\gamma}, \alpha\right) = \left(\frac{\alpha\gamma}{\overline{\gamma}(\alpha-1)}\right)^L. \tag{16}$$

We see how even when using a simple receive strategy as SC, full diversity can be achieved as the diversity order scales with L.

B. CHANNEL CAPACITY

By definition, the normalized average channel capacity [51] is expressed as

$$\overline{C}\left[\text{bps/Hz}\right] = \int_0^\infty \log_2(1+\gamma) f_\gamma(\gamma) d\gamma. \tag{17}$$

Now, replacing (4) in (17), we can evaluate the average capacity. An analytical expression in terms of hypergeometric functions of $_3F_2(\cdot)$ type can be obtained following similar steps as those in [52], or efficiently evaluated numerically using conventional software tools (e.g., MATLAB's function `integral`). Now, similarly to the case with the OP, it is also possible to obtain a simple approximation valid for sufficiently large SNR. Specifically, using the formulation in [53, eq.(8),(9)], a tight lower bound for the average capacity is obtained as

$$\overline{C} \approx \log_2(\overline{\gamma}) - t, \tag{18}$$

with

$$t = -\log_2(e) \frac{d}{dn} \left.\frac{\text{E}\{\gamma^n\}}{\overline{\gamma}^n}\right|_{n=0} \tag{19}$$

$$= -\log_2(e)\left(\log(\alpha-1) - \gamma_e - \Psi(\alpha)\right). \tag{20}$$

The parameter t can be computed from (7) using the chain rule for derivatives, and has dimensions of capacity. Hence, t represents some performance loss with respect to the case with no fading (cfr. Notation in Table 1 for details), for which $t = 0$. As with the OP, a larger α is translated into a better capacity.

The case of SC strategy can also be considered here, by noting that the PDF under SC can be expressed as:

$$f_{\gamma_{\text{SC}}}(\gamma) = L f_\gamma(\gamma) F_\gamma(\gamma)^{L-1}. \tag{21}$$

capacity through (17) can be evaluated.

C. SYMBOL ERROR PROBABILITY

One of the most powerful applications of the MGF is the evaluation of error probabilities in the presence of fading. Simon and Alouini's MGF-approach to the analysis of symbol error probability (SEP) [38] is one of the cornerstones of communication theory. With this approach, the SEP of virtually all modern modulation schemes can be expressed in terms of the MGF of the underlying fading distribution.

As a simple application example, for the specific case of binary differential phase-shift keying (BDPSK), the SEP under $\mathcal{L}_x$-distributed fading can be expressed in closed-form using

(11) as:

$$\text{SEP}(\overline{\gamma}) = \frac{1}{2}M_\gamma(-1) = \alpha U(1, 1-\alpha, (\alpha-1)\overline{\gamma}). \quad (22)$$

D. COMPOSITE FADING MODELING

So far, we have only considered the case of using the $\mathfrak{L}_x$-distribution to model fast fading. In many cases, the average received power experiences some other sorts of fluctuation caused by macroscopic effects due to obstacles. These are often referred to as shadow fading, or *shadowing*, and occur at different time-scales compared to fading. In this situation, the instantaneous received power in (3) can be reformulated as:

$$W = P_T \overline{S}_T S G, \quad (23)$$

where S is a random process independent of $G = |h|^2$ in charge of modeling the effect of shadowing. For convenience, S is defined as a normalized RV, and its aggregate average effect is captured by $\overline{S}_T$. Hence, the joint effects of S and G over the RV W are usually referred to as *composite* fading.

Classically, S is assumed to follow the log-normal distribution. However, because of the lack of tractability of such distribution, the gamma [54] and inverse-gamma [44] distributions have been proposed as good candidates to replace the log-normal distribution to model shadowing. In the case of the latter, it was recently shown that the PDF of W can be expressed in terms of the G-MGF of the underlying fading distribution of G, i.e.,

$$f_W(u) = \frac{\overline{W}^m(m-1)^m}{u^{m+1}\Gamma(m)}M_G^m\left(\frac{(1-m)\overline{W}}{u}\right), \quad (24)$$

where $m \in \mathbb{R}^+$, $m > 1$ is the shape parameter of the inverse-gamma distribution, and $\overline{W} = P_T \overline{S}_T$. Hence, the compact characterization of the $\mathfrak{L}_x$-distribution in the Laplace domain gives a closed-form expression for (24) through (10).

E. OTHER SCENARIOS.

In the previous subsections, we have exemplified how performance analysis over Lomax fading channels can be conducted in a relatively simple form using state-of-the-art mathematical tools and analytical procedures. However, there are much more scenarios on which performance could be analyzed in a direct-form, thanks to the appealing mathematical properties of the Lomax distribution. These are described as follows:

- *Energy detection:* The detection of unknown signals on noisy environments [55] is relevant in numerous disciplines such as radar, cognitive radio, covert communications and, more recently, in integrated sensing and communications [56]. The key performance indicators to quantify the accuracy of energy-detection architectures in the presence of fading are the detection probability vs false alarm probability, usually referred to as the receiver operating characteristic (ROC) curve [55], and the area under the ROC curve (AUC), as introduced in [57]. Using the mathematical formulations in [58], [59], it is possible to express the detection probability and the AUC metric under any arbitrary distribution, in terms of

the G-MGF of the underlying fading channel. Hence, the problem can be directly solved for the case of Lomax fading using the results in Lemma 5.

- *Physical layer security:* The transmission of confidential data between two legitimate peers over a wireless channel, in the presence of a malicious eavesdropper, is a key problem in communication theory ever since the original work formulated in [60]. The characterization of the outage probability of the secrecy capacity, under very general and mild assumptions, is related to the Laplace-domain statistics of the underlying fading channel [41], [61]. Hence, the physical-layer security performance under Lomax fading can be again analyzed using the MGF and G-MGF expressions derived in this work.

- *Outage probability in interference-limited scenarios:* The characterization of the OP in the presence of any arbitrary number of interfering signals is related to the derivatives of the MGF of the fading channel distribution [62]. This corresponds to the G-MGF for integer n, so that the OP formulation in interference-limited regimes under Lomax fading can be straightforwardly obtained using the results in Lemma 5.

- *Generation of white samples:* The generation of random samples from a target distribution is key for empirically validating statistical results using Monte Carlo (MC) simulations, and a first step towards the generation of correlated random sequences [63]. The use of the inverse transformation method is reportedly more efficient than other alternatives based on acceptance-rejection methods [49], [64], but it is only possible when the CDF is invertible. Hence, the closed-form expression for the ICDF in (9) facilitates this task compared to other alternatives in the literature.

IV. NUMERICAL RESULTS

In this section, we evaluate some of the performance metrics previously derived. Where necessary, MC simulations have been included, as a sanity check to validate the theoretical expressions. In different instances, the case of Rayleigh fading has been included for benchmarking purposes.

A. LOMAX STATISTICS

First, we evaluate in Fig. 1 the PDF of the $\mathfrak{L}_x$-distribution for several values of α. The parameter $\overline{\gamma}$ is set to one, for simplicity. In all instances, we double-checked that the PDFs integrate to one. Note that for large values of α (i.e., milder fading severity), the $\mathfrak{L}_x$ PDF tends to behave similar to the exponential distribution (i.e., the distribution of the SNR under Rayleigh fading). Conversely, as α is reduced (i.e., larger fading severity), then the likelihood of smaller SNR values is increased.

In Fig. 2, the AoF is represented as a function of the parameter α. Recall that the AoF is defined only for $\alpha > 2$. We confirm the role of the parameter α to capture the fading severity, as the AoF is inversely proportional to α. Note that,
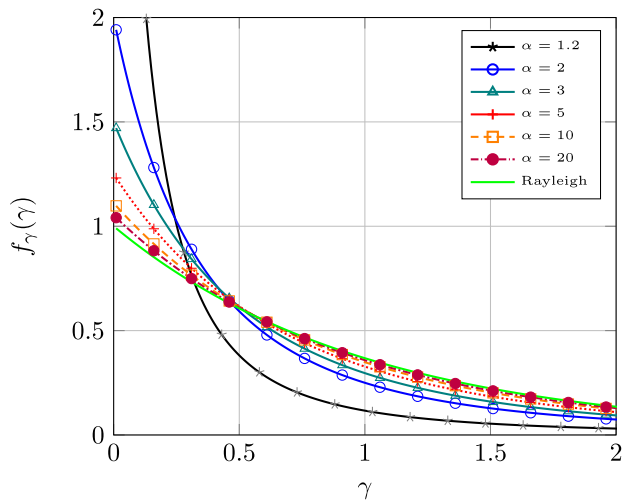
FIGURE 1. $\mathfrak{L}_x$ PDF for different values of α. The case of Rayleigh fading is used for benchmarking purposes (solid green line). Markers denote MC simulations.
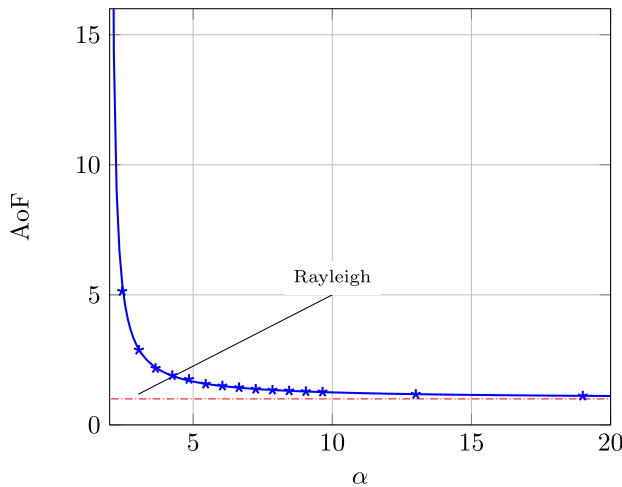

FIGURE 2. $\mathfrak{L}_x$ AoF for different values of α. The case of Rayleigh fading is used for benchmarking purposes (dashed red line). Markers denote MC simulations.

FIGURE 3. $\mathfrak{L}_x$ G-MGF for different values of α and n, as a function of s. Markers denote MC simulations.

FIGURE 4. OP vs. $\overline{\gamma}$ under $\mathfrak{L}_x$ fading for different values of α. The case of Rayleigh fading is used for benchmarking purposes. Dashed lines correspond to the asymptotic expression in (13).

for finite α, the AoF for $\mathfrak{L}_x$ fading is always larger than that of the Rayleigh case. Hence, this implies that the $\mathfrak{L}_x$ distribution is hyper-Rayleigh in the AoF sense [65].

In Fig. 3, the validity of the G-MGF expression in 10 is confirmed. We note that such G-MGF is not only restricted to integer values of the shape parameter, as it is often the case for other distributions [39]. We see how for a given α and a larger negative s, the evaluation of the G-MGF yields a smaller value as n grows. This is translated into a smaller value of a probability measure, e.g., a smaller error probability. A similar conclusion is obtained for a fixed n as α grows (i.e., as fading severity is reduced).

B. OUTAGE PROBABILITY
In Fig. 4, we study the OP under $\mathfrak{L}_x$ fading, once again considering different values of the parameter α. We first consider
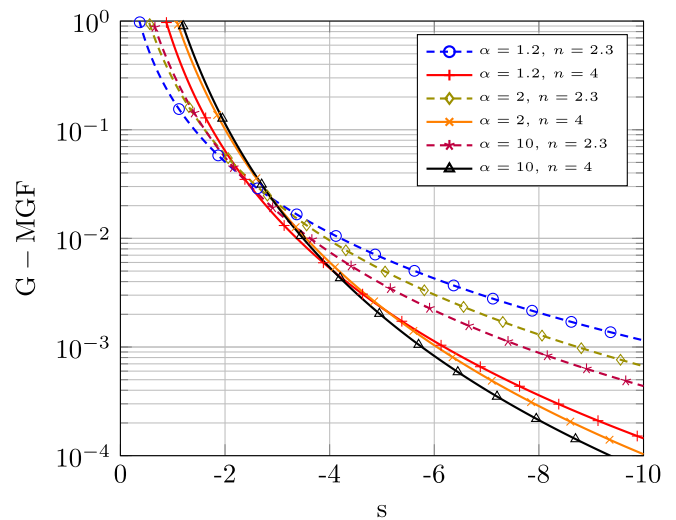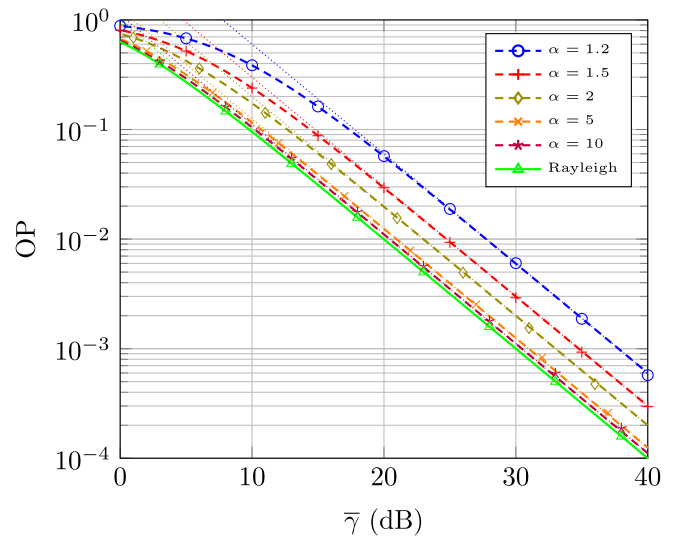
the case of single branch reception, and we set the threshold $\gamma_{\text{th}} = 1$ (i.e., 0 dB). We observe that for larger values of α, the OP is improved (as confirmed by theory). The Rayleigh case serves as a lower bound of performance for sufficiently large α; hence, the $\mathfrak{L}_x$ distribution is also hyper-Rayleigh in the OP sense [65]. We also see that the asymptotic OP tightly matches the exact one in the high-SNR regime. The case of using a larger number of receive branches and a SC strategy is evaluated in Fig. 5. Solid and dashed lines denote the cases of milder ($\alpha = 10$) and more severe ($\alpha = 1.2$) fading, respectively. Dotted lines indicate the asymptotic values of the OP. As predicted by theory, the SC scheme achieves full diversity, so that the asymptotic decay is now proportional to L, the number of receive branches.
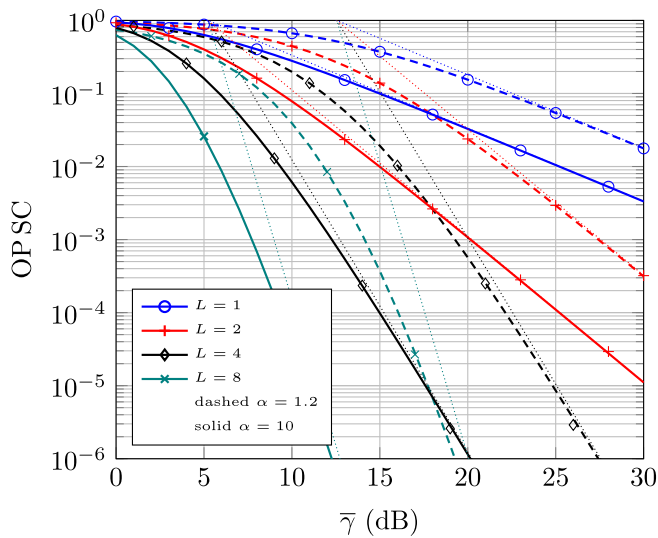
FIGURE 5. OP vs. $\overline{\gamma}$ under $\mathfrak{L}_x$ fading using SC reception, for different values of α and L. Dashed lines correspond to the asymptotic expression in (16).
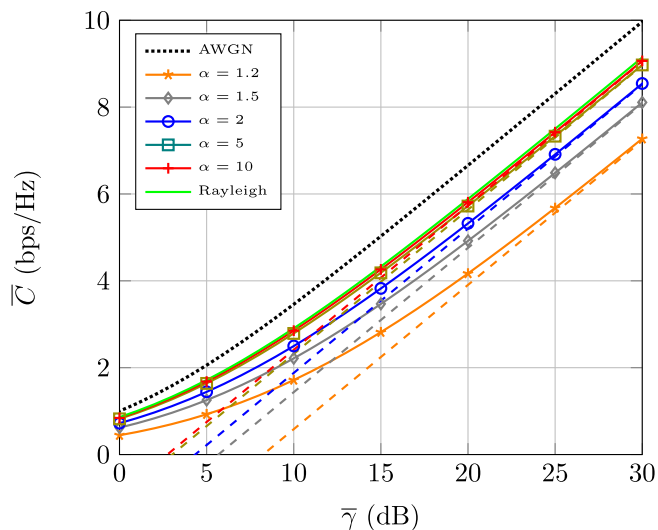

FIGURE 7. Capacity gain $\Delta\overline{C}$ of SC schemes vs. average SNR per branch, for different values of α and L.

FIGURE 6. Average capacity vs. $\overline{\gamma}$ under $\mathfrak{L}_x$ fading for different values of α. The cases of Rayleigh fading and no fading (AWGN) are included for benchmarking purposes. Dashed lines correspond to the asymptotic expression in (18).

FIGURE 8. SEP vs. $\overline{\gamma}$ under $\mathfrak{L}_x$ fading for different values of α.

C. CHANNEL CAPACITY

We now evaluate the average in Fig. 6 for different values of α, considering the case of single branch reception. The Rayleigh and AWGN (i.e., no fading) cases are included for reference purposes. As α grows, then the capacity also grows and tends to that of the Rayleigh case – but always remains far from the AWGN reference. Similarly, as α is decreased then the the capacity is reduced, exhibiting a large performance gap compared to the Rayleigh case. In all instances, we observe that the capacity under $\mathfrak{L}_x$-distributed fading is always lower than that of the Rayleigh case for finite α. Thus, the $\mathfrak{L}_x$ distribution exhibits hyper-Rayleigh behavior in the capacity sense [65].
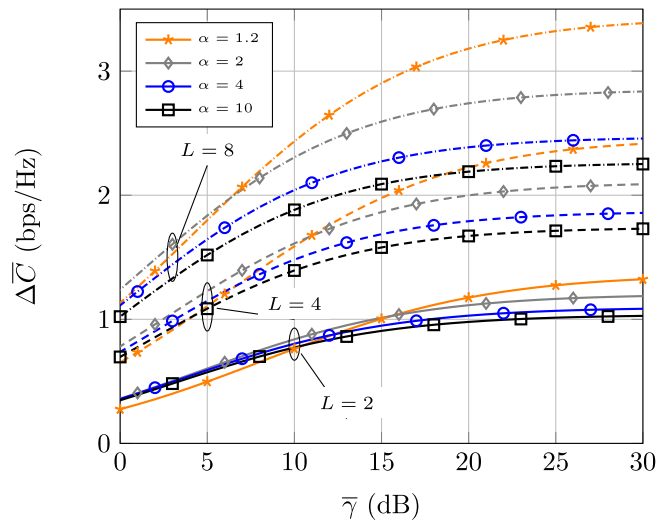
In Fig. 7, we analyze the capacity increase due to the use of SC strategy, for different values of L and α. For the sake of clarity, we represent the metric $\Delta\overline{C} \triangleq \overline{C}_{SC}(\overline{\gamma}, L) - \overline{C}_{SC}(\overline{\gamma}, 1)$, i.e., the capacity gain due to the diversity scheme, with respect to the case of no diversity. First, we observe an intuitive behavior as the capacity gain increases with L, regardless of the SNR regime. We also see that the capacity gain becomes more noticeable in the high-SNR regime when fading is more severe (i.e., for lower α). This confirms the importance of diversity schemes as fading countermeasures, especially in the event of deep fades.

D. SYMBOL ERROR PROBABILITY

It is now time to analyze the error performance under $\mathfrak{L}_x$-distributed fading. As described in Section III-C, we use the case of binary DPSK for exemplary purposes. In Fig. 8, we
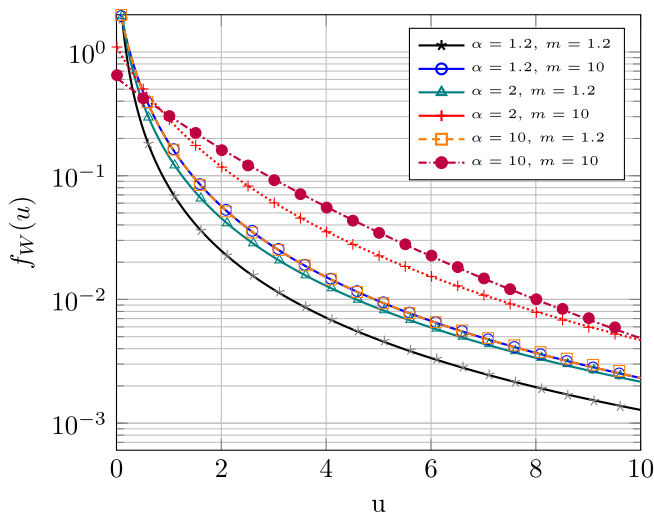
FIGURE 9. PDF of the inverse-gamma based composite fading model, for different m and α. $\overline{W} = 2$ is considered.

represent the SEP (in this case, coincident also with the bit error probability) for different values of α, by direct evaluation of (22). We observe a similar trend as in Fig. 4, i.e., the error probability is larger as α is reduced, and it decays with unity slope regardless of α.

E. COMPOSITE FADING

Finally, we exemplify the flexibility of the $\mathfrak{L}_x$ distribution to extend its behavior to model composite fading. We consider that the shadow fading power coefficient S is inverse-gamma distributed, and the fast fading power coefficient G is $\mathfrak{L}_x$-distributed. Hence, the joint PDF is given by (24), and depicted in Fig. 9 for several values of m (shadowing severity parameter) and α (fading severity parameter). We use a log-scale for the PDF, for the sake of a better representation. We see that increasing the overall composite fading severity, i.e. reducing m or α, makes lower values more likely. However, we see that the values of m and α are not directly exchangeable, confirming the different characteristics of the $\mathfrak{L}_x$ distribution compared to the inverse-gamma one.

V. CONCLUSION

We assessed the use of the $\mathfrak{L}_x$ (Lomax) distribution for wireless channel modeling, by means of a redefinition of its parameters. Closed-form expressions for its fundamental statistics are given, which are then used to evaluate the performance of wireless communication systems in fading channels. We confirmed that the shape parameter α captures fading severity. When jointly considering the OP, capacity and AoF, we can conclude that the $\mathfrak{L}_x$-distribution has *full* hyper-Rayleigh behavior according to the categorization in [65]. Hence, it can reproduce more severe conditions compared to Rayleigh fading.

The Lomax distribution has been identified to be relevant in a number of practical situations and use cases, including D2D,

URLLC, or cognitive radio networks, among others, which justify the interest in pursuing the statistical characterization of such a distribution. This serves as a stepping stone that motivates further research actions, including additional activities and campaigns destined to providing empirical evidences that support the relevance of the Lomax distribution in different contexts.

REFERENCES

[1] I. Sánchez and F. J. López-Martínez, "The lomax distribution for wireless channel modeling: A preliminary study," in *Proc. IEEE 7th Ecuador Tech. Chapters Meeting*, 2023, pp. 1–4.

[2] L. Tsang, J. A. Kong, and K.-H. Ding, *Scattering of Electromagnetic Waves: Theories and Applications*. Hoboken, NJ, USA: Wiley, 2004.

[3] S. O. Rice, "Distribution of the duration of fades in radio transmission: Gaussian noise model," *Bell Syst. Tech. J.*, vol. 37, no. 3, pp. 581–635, 1958.

[4] M. Nakagami, "The M-distribution–A general formula of intensity distribution of rapid fading," in *Proc. Stat. Methods Radio Wave Propag.*, 1960, pp. 3–36.

[5] P. Beckmann, "Statistical distribution of the amplitude and phase of a multiply scattered field," *J. Res. Nat. Bur. Stand.-D. Radio Propag.*, vol. 66D, no. 3, pp. 231–240, 1962.

[6] M. D. Yacoub, "The κ-μ distribution and the η-μ distribution," *IEEE Antennas Propag. Mag.*, vol. 49, no. 1, pp. 68–81, Feb. 2007.

[7] M. D. Yacoub, "The α-μ distribution: A physical fading model for the stacy distribution," *IEEE Trans. Veh. Technol.*, vol. 56, no. 1, pp. 27–34, Jan. 2007.

[8] J. F. Paris, "Statistical characterization of κ-μ shadowed fading," *IEEE Trans. Veh. Technol.*, vol. 63, no. 2, pp. 518–526, Feb. 2014.

[9] S. K. Yoo, S. L. Cotton, P. C. Sofotasios, M. Matthaiou, M. Valkama, and G. K. Karagiannidis, "The fisher-snedecor $\mathcal{F}$ distribution: A simple and accurate composite fading model," *IEEE Commun. Lett.*, vol. 21, no. 7, pp. 1661–1664, Jul. 2017.

[10] G. D. Durgin, T. S. Rappaport, and D. A. de Wolf, "New analytical models and probability density functions for fading in wireless communications," *IEEE Trans. Commun.*, vol. 50, no. 6, pp. 1005–1015, Jun. 2002.

[11] J. M. Romero-Jerez, F. J. Lopez-Martinez, J. P. Peña-Martín, and A. Abdi, "Stochastic fading channel models with multiple dominant specular components," *IEEE Trans. Veh. Technol.*, vol. 71, no. 3, pp. 2229–2239, Mar. 2022.

[12] J. M. Romero-Jerez, F. J. Lopez-Martinez, J. F. Paris, and A. J. Goldsmith, "The fluctuating two-ray fading model: Statistical characterization and performance analysis," *IEEE Trans. Wireless Commun.*, vol. 16, no. 7, pp. 4420–4432, Jul. 2017.

[13] M. Olyaee, J. M. Romero-Jerez, F. J. Lopez-Martinez, and A. J. Goldsmith, "Alternative formulations for the fluctuating two-ray fading model," *IEEE Trans. Wireless Commun.*, vol. 21, no. 11, pp. 9404–9416, Nov. 2022.

[14] M. Olyaee, J. A. Cortés, F. J. Lopez-Martinez, J. F. Paris, and J. M. Romero-Jerez, "The fluctuating two-ray fading model with independent specular components," *IEEE Trans. Veh. Technol.*, vol. 72, no. 5, pp. 5533–5545, May 2023.

[15] S. L. Cotton, "Human body shadowing in cellular device-to-device communications: Channel modeling using the shadowed κ-μ fading model," *IEEE J. Sel. Areas Commun.*, vol. 33, no. 1, pp. 111–119, Jan. 2015.

[16] L. Moreno-Pozas, F. J. Lopez-Martinez, S. L. Cotton, J. F. Paris, and E. Martos-Naya, "Comments on "human body shadowing in cellular device-to-device communications: Channel modeling using the shadowed $\kappa - \mu$ fading model"," *IEEE J. Sel. Areas Commun.*, vol. 35, no. 2, pp. 517–520, Feb. 2017.

[17] P. Ramirez-Espinosa, F. J. Lopez-Martinez, J. F. Paris, M. D. Yacoub, and E. Martos-Naya, "An extension of the κ-μ shadowed fading model: Statistical characterization and applications," *IEEE Trans. Veh. Technol.*, vol. 67, no. 5, pp. 3826–3837, May 2018.

[18] L. Moreno-Pozas, F. J. Lopez-Martinez, J. F. Paris, and E. Martos-Naya, "The κ-μ shadowed fading model: Unifying the κ-μ and η-μ distributions," *IEEE Trans. Veh. Technol.*, vol. 65, no. 12, pp. 9630–9641, Dec. 2016.

[19] M. D. Yacoub, "The α-η-κ-μ fading model," *IEEE Trans. Antennas Propag.*, vol. 64, no. 8, pp. 3597–3610, Aug. 2016.

[20] H. Hashemi, "The indoor radio propagation channel," *Proc. IEEE*, vol. 81, no. 7, pp. 943–968, Jul. 1993.

[21] F. Babich and G. Lombardi, "Statistical analysis and characterization of the indoor propagation channel," *IEEE Trans. Commun.*, vol. 48, no. 3, pp. 455–464, Mar. 2000.

[22] S. K. Yoo, S. L. Cotton, L. Zhang, and P. C. Sofotasios, "The inverse gamma distribution: A new shadowing model," in *Proc. IEEE 8th Asia-Pacific Conf. Antennas Propag.*, 2019, pp. 475–476.

[23] N. Simmons, C. R. N. D. Silva, S. L. Cotton, P. C. Sofotasios, S. K. Yoo, and M. D. Yacoub, "On shadowing the κ-μ fading model," *IEEE Access*, vol. 8, pp. 120513–120536, 2020.

[24] I. Sánchez and F. J. López-Martínez, "A formulation of the log-logistic distribution for fading channel modeling," *Electron.*, vol. 11, no. 15, 2022, Art. no. 2409.

[25] D. K. Wilson, C. R. Hart, C. L. Pettit, D. J. Breton, E. T. Nykaza, and V. E. Ostashev, "Scattered signal distributions, parametric uncertainties, and Bayesian sequential updating," in *Proc. Meetings Acoust.*, 2017, Art. no. 055002 .

[26] D. K. Wilson, D. J. Breton, C. R. Hart, V. E. Ostashev, E. T. Nykaza, and C. L. Pettit, "Impact of parametric uncertainties on scattered signal distributions and receiver operating characteristics," Tech. Rep. (Eng. Res. Develop. Center, U.S.), ERDC TR-18-7, 2018.

[27] T. Kallehauge, P. Ramirez-Espinosa, A. E. Kalør, and P. Popovski, *Statistical Characterization of URLLC : Frequentist and Bayesian Approaches*. Hoboken, NJ, USA: Wiley, 2023, ch. 2, pp. 15–59.

[28] A. S. Daghal and Q. Z. Ahmed, "Video content delivery using multiple devices to single device communications," in *Proc. IEEE 83rd Veh. Technol. Conf.*, 2016, pp. 1–5.

[29] A. S. Daghal, H. Zhu, and J. Wang, "Content delivery analysis in multiple devices to single device communications," *IEEE Trans. Veh. Technol.*, vol. 67, no. 11, pp. 10218–10231, Nov. 2018.

[30] S. Nadarajah and S. Kotz, "Expressions for bit error probability," *Wireless Commun. Mobile Comput.*, vol. 8, no. 7, pp. 885–894, 2008.

[31] X.-L. Huang, F. Hu, J. Wu, H.-H. Chen, G. Wang, and T. Jiang, "Intelligent cooperative spectrum sensing via hierarchical Dirichlet process in cognitive radio networks," *IEEE J. Sel. Areas Commun.*, vol. 33, no. 5, pp. 771–787, May 2015.

[32] X.-L. Huang, J. Wu, W. Li, Z. Zhang, F. Zhu, and M. Wu, "Historical spectrum sensing data mining for cognitive radio enabled vehicular ad-hoc networks," *IEEE Trans. Dependable Secure Comput.*, vol. 13, no. 1, pp. 59–70, Jan/Feb. 2016.

[33] O. L. Alcaraz López, H. Alves, and M. Latva-Aho, "Rate control under finite blocklength for downlink cellular networks with reliability constraints," in *Proc. IEEE 15th Int. Symp. Wireless Commun. Syst.*, 2018, pp. 1–6.

[34] O. L. Alcaraz López, H. Alves, and M. Latva-aho, "Joint power control and rate allocation enabling ultra-reliability and energy efficiency in SIMO wireless networks," *IEEE Trans. Commun.*, vol. 67, no. 8, pp. 5768–5782, Aug. 2019.

[35] M. Abramowitz and I. A. Stegun, *Handbook of Mathematical Functions With Formulas, Graphs, and Mathematical Tables*, 10th ed. Washington DC, USA: US Dept. of Commerce, Nat. Bur. Standards, 1972.

[36] I. S. Gradshteyn and I. M. Ryzhik, *Table of Integrals, Series and Products*. San Diego, CA, USA: Academic Press, 2007.

[37] K. S. Lomax, "Business failures: Another example of the analysis of failure data," *J. Amer. Statist. Assoc.*, vol. 49, no. 268, pp. 847–852, 1954.

[38] M. K. Simon and M.-S. Alouini, *Digital Communication Over Fading Channels*, vol. 95. Hoboken, NJ, USA: Wiley, 2005.

[39] J. P. Peña-Martín, J. M. Romero-Jerez, and F. J. Lopez-Martinez, "Generalized MGF of the two-wave with diffuse power fading model with applications," *IEEE Trans. Veh. Technol.*, vol. 67, no. 6, pp. 5525–5529, Jun. 2018.

[40] J. Gong, H. Lee, and J. Kang, "Generalized MGF of inverse Gaussian distribution with applications to wireless communications," *IEEE Trans. Veh. Technol.*, vol. 69, no. 2, pp. 2332–2336, Feb. 2020.

[41] G. Gomez, F. J. Lopez-Martinez, D. Morales-Jimenez, and M. R. McKay, "On the equivalence between interference and eavesdropping in wireless communications," *IEEE Trans. Veh. Technol.*, vol. 64, no. 12, pp. 5935–5940, Dec. 2015.

[42] J. P. Peña-Martín, J. M. Romero-Jerez, and F. J. Lopez-Martinez, "Generalized MGF of beckmann fading with applications to wireless communications performance analysis," *IEEE Trans. Commun.*, vol. 65, no. 9, pp. 3933–3943, Sep. 2017.

[43] M. Di Renzo, F. Graziosi, and F. Santucci, "Channel capacity over generalized fading channels: A novel MGF-Based approach for performance analysis and design of wireless communication systems," *IEEE Trans. Veh. Technol.*, vol. 59, no. 1, pp. 127–149, Jan. 2010.

[44] P. Ramírez-Espinosa and F. J. López-Martínez, "Composite fading models based on inverse gamma shadowing: Theory and validation," *IEEE Trans. Wireless Commun.*, vol. 20, no. 8, pp. 5034–5045, Aug. 2021.

[45] J. M. Romero-Jerez and F. J. Lopez-Martinez, "A new framework for the performance analysis of wireless communications under Hoyt (Nakagami- q) fading," *IEEE Trans. Inf. Theory*, vol. 63, no. 3, pp. 1693–1702, Mar. 2017.

[46] J. Reig, V. M. Rodrigo Peñarrocha, L. Rubio, M. T. Martínez-Inglés, and J. M. Molina-García-Pardo, "The folded normal distribution: A new model for the small-scale fading in line-of-sight (LOS) condition," *IEEE Access*, vol. 7, pp. 77328–77339, 2019.

[47] N. D. Chatzidiamantis, H. G. Sandalidis, G. K. Karagiannidis, and M. Matthaiou, "Inverse Gaussian modeling of turbulence-induced fading in free-space optical systems," *IEEE J. Light. Technol.*, vol. 29, no. 10, pp. 1590–1596, May 2011.

[48] F. J. Lopez-Martinez, D. Morales-Jimenez, E. Martos-Naya, and J. F. Paris, "On the bivariate Nakagami-m cumulative distribution function: Closed-form expression and applications," *IEEE Trans. Commun.*, vol. 61, no. 4, pp. 1404–1414, Apr. 2013.

[49] F. J. Lopez-Martinez, L. Moreno-Pozas, and E. Martos-Naya, "Novel results for the κ-μ extreme fading distribution: Generation of white samples and capacity analysis," *IEEE Commun. Lett.*, vol. 19, no. 9, pp. 1580–1583, Sep. 2015.

[50] Z. Wang and G. Giannakis, "A simple and general parameterization quantifying performance in fading channels," *IEEE Trans. Commun.*, vol. 51, no. 8, pp. 1389–1398, Aug. 2003.

[51] A. J. Goldsmith and P. P. Varaiya, "Capacity of fading channels with channel side information," *IEEE Trans. Inf. Theory*, vol. 43, no. 6, pp. 1986–1992, Nov. 1997.

[52] S. K. Yoo et al., "A comprehensive analysis of the achievable channel capacity in $\mathcal{F}$ composite fading channels," *IEEE Access*, vol. 7, pp. 34078–34094, 2019.

[53] F. Yilmaz and M. S. Alouini, "Novel asymptotic results on the high-order statistics of the channel capacity over generalized fading channels," in *Proc. IEEE 13th Int. Workshop Signal Process. Adv. Wireless Commun.*, 2012, pp. 389–393.

[54] A. Abdi and M. Kaveh, "A comparative study of two shadow fading models in ultrawideband and other wireless systems," *IEEE Trans. Wireless Commun.*, vol. 10, no. 5, pp. 1428–1434, May 2011.

[55] H. Urkowitz, "Energy detection of unknown deterministic signals," *Proc. IEEE*, vol. 55, no. 4, pp. 523–531, Apr. 1967.

[56] H. Wymeersch et al., "Integration of communication and sensing in 6G: A joint industrial and academic perspective," in *Proc. IEEE 32nd Annu. Int. Symp. Pers., Indoor, Mobile Radio Commun.*, 2021, pp. 1–7.

[57] S. Atapattu, C. Tellambura, and H. Jiang, "Analysis of area under the ROC curve of energy detection," *IEEE Trans. Wireless Commun.*, vol. 9, no. 3, pp. 1216–1225, Mar. 2010.

[58] A. Annamalai, O. Olabiyi, S. Alam, O. Odejide, and D. Vaman, "Unified analysis of energy detection of unknown signals over generalized fading channels," in *Proc. IEEE 7th Int. Wireless Commun. Mobile Comput. Conf.*, 2011, pp. 636–641.

[59] O. Olabiyi, S. Alam, O. Odejide, and A. Annamalai, "Efficient evaluation of area under the ROC curve of energy detectors over fading channels," in *Proc. 14th ACM Int. Conf. Model., Anal. Simul. Wireless Mobile Syst.*, New York, NY, USA, 2011, pp. 261–264.

[60] M. Bloch, J. Barros, M. R. D. Rodrigues, and S. W. McLaughlin, "Wireless information-theoretic security," *IEEE Trans. Inf. Theory*, vol. 54, no. 6, pp. 2515–2534, Jun. 2008.

[61] J. M. Romero-Jerez, G. Gomez, and F. J. Lopez-Martinez, "On the outage probability of secrecy capacity in arbitrarily-distributed fading channels," in *Proc. IEEE 21th Eur. Wireless Conf.*, 2015, pp. 1–6.

[62] J. M. Romero-Jerez and A. J. Goldsmith, "Receive antenna array strategies in fading and interference: An outage probability comparison," *IEEE Trans. Wireless Commun.*, vol. 7, no. 3, pp. 920–932, Mar. 2008.

[63] R. Cogliatti, R. A. A. de Souza, and M. D. Yacoub, "Practical, highly efficient algorithm for generating κ-μ and η-μ variates and a Near-100% efficient algorithm for generating α-μ variates," *IEEE Commun. Lett.*, vol. 16, no. 11, pp. 1768–1771, Nov. 2012.

[64] V. M. Rennó, R. A. A. de Souza, and M. D. Yacoub, "On the generation of white samples in severe fading conditions," *IEEE Commun. Lett.*, vol. 23, no. 1, pp. 180–183, Jan. 2019.

[65] C. Garcia-Corrales, U. Fernandez-Plazaola, F. J. Cañete, J. F. Paris, and F. J. Lopez-Martinez, "Unveiling the hyper-Rayleigh regime of the fluctuating two-ray fading model," *IEEE Access*, vol. 7, pp. 75367–75377, 2019.

F. JAVIER LÓPEZ-MARTÍNEZ (Senior Member, IEEE) received the M.Sc. and Ph.D. degrees in telecommunication engineering from the University of Malaga, Málaálaga, Spain, in 2005 and 2010, respectively. He was a Marie Curie Postdoctoral Fellow with the Wireless Systems Lab, Stanford University, Stanford, CA, USA, between 2012 and 2014. He was a Visiting Researcher with the University College London, London, U.K., in 2010, and Queen's University Belfast, Belfast, Northern Ireland, in 2018. He is an Associate Professor (on leave) with the Communication Engineering Department, University of Malaga, and an EMERGIA Research Professor with the Department of Signal Theory, Networking and Communications, University of Granada, Granada, Spain. He was the recipient of several research awards, including the Best Paper Award from the Communication Theory Symposium at the IEEE Globecom 2013, the Outstanding Service Award by the IEEE Communication Theory Technical Committee in 2022, and Exemplary Reviewer Certificates for IEEE Communications Letters (2014, 2019), IEEE Transactions on Communications (2014, 2016, 2019), and IEEE Wireless Communications Letters (2021). He has been an Editor of IEEE TRANSACTIONS ON COMMUNICATIONS in the area of wireless communications, between 2017 and 2022. Since 2023, he has been an Editor of IEEE TRANSACTIONS ON INFORMATION FORENSICS AND SECURITY. His research interests include wireless channel modeling, physical layer security, and signal processing for communications.

IVAN SÁNCHEZ received the degree in electronic and telecommunication engineering from Escuela Politécnica Nacional, Quito, Ecuador, in 2006, and the M.Sc. degree from Universidad Central del Ecuador, Quito, in 2015. He is currently working toward the Ph.D. degree in the Telecommunication Engineering Doctorate program with Universidad de Málaga, Málaálaga, Spain, and is an associate professor with Universidad de las Américas, Quito. He was the recipient of the best paper award in the communications track at IEEE ETCM 2023. His research interests include wireless channel modeling and 6G communications.